Received: 2 February 2017 | Accepted: 3 February 2017

DOI 10.1002/jcp.25843

ORIGINAL RESEARCH ARTICLE

WILEY Journal of Cellular Physiology

NMDA receptor subunit composition controls dendritogenesis of hippocampal neurons through CAMKII, CREB-P, and H3K27ac

Fernando J. Bustos[1,2] | Nur Jury[1] | Pablo Martinez[1] | Estibaliz Ampuero[1] | Matias Campos[1] | Sebastian Abarzúa[1] | Karen Jaramillo[1,2] | Susanne Ibing[3] | Muriel D. Mardones[1] | Henny Haensgen[4] | Julia Kzhyshkowska[3] | Maria Florencia Tevy[5] | Rachael Neve[4] | Magdalena Sanhueza[6] | Lorena Varela-Nallar[1] | Martín Montecino[1,2] | Brigitte van Zundert[1]

[1] Center for Biomedical Research, Faculty of Biological Sciences and Faculty of Medicine, Universidad Andres Bello, Santiago, Chile

[2] FONDAP Center for Genome Regulation, Santiago, Chile

[3] Institute of Transfusion Medicine and Immunology, Medical Faculty Mannheim, University of Heidelberg, German Red Cross Blood Service Baden-Württemberg—Hessen, Mannheim, Germany

[4] Department of Brain and Cognitive Sciences, Massachusetts Institute of Technology, Cambridge, Massachusetts

[5] Centro de Genómica y Bioinformática, Facultad de Ciencias, Universidad Mayor, Santiago, Chile

[6] Department of Biology, Faculty of Sciences, University of Chile, Santiago, Chile

Correspondence
Brigitte van Zundert, PhD, Center for Biomedical Research, Faculty of Biological Sciences and Faculty of Medicine, Universidad Andres Bello, Avenida Republica 217, Santiago, Chile.
Email: bvanzundert@unab.cl

Funding information
FONDECYT, Grant number: 1140301; FONDECYT, Grant number: 1101012; UNAB Núcleus, Grant number: DI-603-14N; DRI USA, Grant number: 2013–0030; FP7-PEOPLE-2011-IRSES, Grant number: 295185; FONDEQUIP EQM, Grant number: 140166; CONICYT, Grant number: 24110099; CONICYT, Grant number: 201161486; FONDECYT, Grant number: 3130582; CONICYT, Grant number: 21151563; CONICYT, Grant number: 21151265; FONDECYT, Grant number: 11130203; FONDECYT, Grant number: 1140700; FONDECYT, Grant number: 1150933; FONDAP, Grant number: 15090007; FONDECYT, Grant number: 1130706

Dendrite arbor growth, or dendritogenesis, is choreographed by a diverse set of cues, including the NMDA receptor (NMDAR) subunits NR2A and NR2B. While NR1NR2B receptors are predominantly expressed in immature neurons and promote plasticity, NR1NR2A receptors are mainly expressed in mature neurons and induce circuit stability. How the different subunits regulate these processes is unclear, but this is likely related to the presence of their distinct C-terminal sequences that couple different signaling proteins. Calcium-calmodulin-dependent protein kinase II (CaMKII) is an interesting candidate as this protein can be activated by calcium influx through NMDARs. CaMKII triggers a series of biochemical signaling cascades, involving the phosphorylation of diverse targets. Among them, the activation of cAMP response element-binding protein (CREB-P) pathway triggers a plasticity-specific transcriptional program through unknown epigenetic mechanisms. Here, we found that dendritogenesis in hippocampal neurons is impaired by several well-characterized constructs (i.e., NR2B-RS/QD) and peptides (i.e., tatCN21) that specifically interfere with the recruitment and interaction of CaMKII with the NR2B C-terminal domain. Interestingly, we found that transduction of NR2AΔIN, a mutant NR2A construct with increased interaction to CaMKII, reactivates dendritogenesis in mature hippocampal neurons in vitro and in vivo. To gain insights into the signaling and epigenetic mechanisms underlying NMDAR-mediated dendritogenesis, we used immunofluorescence staining to detect CREB-P and acetylated lysine 27 of histone H3 (H3K27ac), an activation-associated histone tail mark. In contrast to control mature neurons, our data shows that activation of the NMDAR/CaMKII/ERK-P/CREB-P signaling axis in neurons expressing NR2AΔIN is not correlated with increased nuclear H3K27ac levels.

KEYWORDS
brain, CaMKII, cultures, dendrites, H3K27Ac, histone modification, neuron, NMDAR, spines

1 | INTRODUCTION

During the first weeks of postnatal brain development, dynamic and large-scale morphological changes occur to generate a connective network. These changes include dendrite formation as well as pruning to eliminate excessive and mis-targeted branches (Cline & Haas, 2008; Jan & Jan, 2010). With maturation, and depending on sensory, motor, and cognitive stimuli, dendritic branches stabilize, and form the foundation of the mature neuronal circuitry (Chow et al., 2009; Koleske, 2013).

Through developmental and coordinated synaptic activities, dendritic branches acquire dendritic protrusions, and spines that harbor synapses. Accumulating evidence indicates that limited dendritic arbor complexity, and consequently reduced synaptic connectivity, plays an important role in the cognitive and memory impairments observed with aging and in a number of neurological and cognitive disorders, such as depression, Alzheimer's disease, schizophrenia, and stroke, among others (Kulkarni & Firestein, 2012). Elucidating the molecular underpinnings of dendrite dynamics, outgrowth, and stabilization might allow for the reactivation of dendritogenesis. This reactivation could promote synaptic connectivity in aging persons and adult patients with brain disorders.

Excitatory synapses can hold hundreds of proteins in the postsynaptic density (PSD) including N-methyl-D-aspartate receptors (NMDARs), which together with (α-amino-3-hydroxy-5-methyl-4-isoxazolepropionic acid receptors (AMPARs) are the primary recipients of excitatory inputs (Sheng & Kim, 2011). A critical role for NMDARs has been established in neuronal circuit development and long-term potentiation (LTP) of synaptic strength (Cline & Haas, 2008), a cellular model of memory acquisition (Martin, Grimwood, & Morris, 2000). NMDARs are composed of two obligatory NR1 subunits plus two variable NR2A-D and/or NR3A-B subunits. Considerable evidence points to a central role of the NR2A and NR2B subunits in regulating diverse forms of structural and functional plasticity (Cull-Candy & Leszkiewicz, 2004; Foster et al., 2010; van Zundert, Yoshii, & Constantine-Paton, 2004).

During the postnatal development of several brain regions, including the well-studied hippocampus, NMDARs undergo an activity-dependent subunit switch from NR2B- to NR2A-rich containing NMDARs (Al-Hallaq, Conrads, Veenstra, & Wenthold, 2007; Alvarez, Ridenour, & Sabatini, 2007; Bustos et al., 2014; Yashiro & Philpot, 2008; van Zundert et al., 2004). The strong correlation between the NR2B-to-NR2A subunit switch and circuit maturation suggests that NR1NR2B-receptors induce dendrite plasticity, whereas NR1NR2A-receptors promote dendrite stability. Indeed, gain-and-loss-of-function studies in a variety of experimental models have shown that synaptic NR2B-rich NMDARs are required for dendrite formation in immature neurons (Bustos et al., 2014; Espinosa, Wheeler, Tsien, & Luo, 2009; Sepulveda et al., 2010). In contrast, synaptic NR2A-NMDARs control structural refinement and dendritic stability (Bustos et al., 2014; Charych et al., 2006; Henriquez et al., 2013).

Despite that dendritic branches stabilize during maturation (Chow et al., 2009; Koleske, 2013), remarkably, dendritogenesis in mature neurons can be robustly reactivated when NR2B-NMDARs are reinserted into the synapse by reducing the synaptic levels of PSD95, a critical scaffolding protein that anchors NR2A-NMDARs at the PSD (Ampuero, Jury, Härtel, Marzolo, & van Zundert, 2017; Bustos et al., 2014; Charych et al., 2006; Henriquez et al., 2013). The precise molecular basis for how NR2B-NMDARs, and not NR2A-NMDARs, induce dendritic outgrowth is currently unknown. The coupling of NR2A and NR2B to specific signaling proteins might explain the contrasting roles of these subunits in controlling structural and functional changes in the neuronal circuitry. Understanding this process would provide insights into the mechanisms underlying learning and memory, as well as brain disorders as stated above.

Over the past 25 years, calmodulin-dependent protein kinase II (CaMKII) has been studied extensively in hippocampal and other neurons as a mediator of plasticity, and learning and memory (Hell, 2014; Lisman, Yasuda, & Raghavachari, 2012). Particularly interesting is the evidence that NMDAR-mediated calcium influx activates CaMKII and subsequently triggers a biochemical signaling cascade that regulates structural and functional plasticity, through activation of the extracellular signaling kinase (ERK) and cAMP response element-binding protein (CREB) pathway (Greer & Greenberg, 2008; Lisman et al., 2012; Sanhueza & Lisman, 2013). The CaMKIIα subunit (hereafter termed CaMKII unless specifically indicated) is a major synaptic protein, comprising 1–2% of the total protein levels. The CaMKII kinase activity is regulated by an intrinsic signaling cascade that involves calcium/calmodulin binding and an autophosphorylation step (Molloy & Kennedy, 1991). NMDAR activity mediates CaMKII translocation to the PSD, where it is maintained through a direct interaction with the C-terminal tail of the NMDAR (Bayer, De Koninck, Leonard, Hell, & Schulman, 2001; Shen & Meyer, 1999). Further studies show that while NR2B efficiently interacts with CaMKII (Barria & Malinow, 2005; Bayer et al., 2001; Gambrill & Barria, 2011; Mayadevi, Praseeda, Kumar, & Omkumar, 2002; Sanhueza et al., 2011), NR2A binds this kinase poorly (Barria & Malinow, 2005; Mayadevi et al., 2002). Additional studies with CaMKII mutant constructs (i.e., NR2B-RS/QD; Barria & Malinow, 2005; Gambrill & Barria, 2011; Mayadevi et al., 2002) or peptides (e.g., tatCN21; Sanhueza et al., 2011) that specifically interfere with NR2B-CaMKII binding have shown that the recruitment and interaction of active CaMKII with the NR2B C-terminal during early development is necessary for spine formation, synapse growth, and LTP.

Diverse gain-and-loss-of-function approaches implicate that CaMKII regulates dendritic outgrowth in several experimental systems, but results are inconsistent (Gaudillière et al., 2004; Ghiretti, Kenny, Marr, & Paradis, 2013; Wu & Cline, 1998). The reasons for these discrepancies are unknown and might depend on the different approaches used to manipulate CaMKII expression and/or function, or, alternatively, on the developmental stage of neurons, subsequently, impacting potential interactions of CaMKII with proteins such as NMDARs. Considering prior work, in this study we hypothesized that the coupling of NR2B-NMDARs to CaMKII is necessary for dendritic growth. Additionally, we proposed that dendritogenesis

could be reactivated in mature neurons when expressing a NR2A mutant construct that exhibits enhanced CaMKII binding. Here we provide the first evidence that depending on the developmental stage of hippocampal neurons the association between CaMKII and NMDARs differentially controls dendritogenesis. Furthermore, we studied the molecular basis of how specific interactions between NMDARs and CaMKII mediate dendritic outgrowth.

2 | MATERIALS AND METHODS

2.1 | Neuronal cultures

All protocols involving rodents were carried out in accordance with NIH guidelines, and were approved by the Ethical and Bio-security Committees of Universidad Andrés Bello. Cultures of hippocampal neurons and motoneurons were prepared, respectively from embryonic day (E) 18 and E14 Sprague-Dawley rat fetuses as previously described (Bustos et al., 2014; Henriquez et al., 2013; Sepulveda et al., 2010). Briefly, pregnant Sprague-Dawley rats were deeply anesthetized with CO_2 and hippocampi or whole spinal cord were removed from fetuses. The dorsal part of the spinal cord was removed and discarded using a small razor blade. Hippocampal and spinal cord tissue was excised and placed into ice-cold PBS containing 50 µg/ml penicillin/streptomycin. The extracts were minced and incubated for 20 min at 37°C in pre-warmed PBS containing 0.25% trypsin and then transferred to a tube containing Dulbecco's modified Eagle's medium supplemented with 10% horse serum and 100 U/ml penicillin/streptomycin. Cells were resuspended by mechanical agitation through fire-polished glass Pasteur pipettes of decreasing diameters. Cells were counted and plated on freshly prepared poly-L-lysine-coated 24-well plates (1 mg/ml; Sigma P2636, St Louis, MO). Two hours after seeding, plating media was replaced by hippocampal growth media Neurobasal (Thermo Fisher Scientific, Carlsbad, CA, USA) supplemented with B27 (Thermo Fisher Scientific, 17504044), 2 mM L-glutamine (Thermo Fisher Scientific, 25030–081), 100 U/ml penicillin/streptomycin (Thermo Fisher Scientific, 15070–063), or ventral spinal cord growth media [70% MEM (Invitrogen 11090–073), 25% Neurobasal media (Thermo Fisher Scientific, 21103–049), 1% N2 supplement (Thermo Fisher Scientific, 17502–048), 1% L-glutamine (Thermo Fisher Scientific, 25030–081), 1% penicillin-streptomycin (Invitrogen 15070–063), 2% horse serum (Hyclone SH30074.03), and 1 mM pyruvate (Sigma)]. All VSCNs cultures were supplemented with 45 g/ml E18 chick leg extract (Henderson et al., 1993). On day 2, neurons were treated with 2 µM cytosine arabinoside for 24 hr, after that growth media was replaced with half of new media every 2–3 days.

2.2 | Constructs and transient transfections

Transfection methodologies differed with cell type and developmental stage. Hippocampal neurons at two, four, and seven DIV and spinal cord neurons at four DIV were transfected by a $CaPO_4$ transfection as previously described (Bustos et al., 2014; Sepulveda et al., 2010). Briefly, hippocampal growth media or ventral spinal cord media was replaced with pre-warmed MEM (Thermo Fisher Scientific, 21103–049) 20 min prior to transfection. DNA/calcium complexes were added to the plates drop wise and incubated for 1 hr at 37°C and 5% CO_2. Cells were washed three times with pre-equilibrated MEM/EBSS at 10% CO_2 for 20 min to dissolve the DNA-$CaPO_4$ precipitates. Cells were left at 37°C and 5% CO_2 until 10–12 DIV to performed morphological analyses.

Hippocampal neurons at 15 DIV were transfected by Magneto-fection™ using the Neuromag protocol according to manufacturer instructions (OZ Biosciences, San Diego, CA) with slight modifications, and as previously described (Ampuero et al., 2017; Bustos et al., 2014; Henriquez et al., 2013). Briefly, 30 min before magnetofection, medium was replaced with pre-warmed Neurobasal media. Plasmid DNA was incubated with Neuromag beads, in a ratio of 500 ng of DNA per 0.75 µl of nanobeads in 100 µl of Neurobasal media. This mixture was added drop wise to each 24-well plate and incubated for 15 min at 37°C over a magnetic plate (OZ Biosciences). Old medium was restored after 45 min. Constructs used to transfect neuronal cultures include a plasmid coding for GFP to visualize neuronal morphology in detail; plasmids to overexpress NMDAR subunits GFP-NR2A and GFP-NR2B (Luo et al., 2002); NMDAR subunits that either impede CaMKII binding to NR2B NR2B-RS/QD or enhance the binding of CamKII to the NR2A subunit NR2AΔIN (Barria & Malinow, 2005); plasmids to knock down the expression of the NMDAR subunit NR2A and NR2B via small short-hairpin RNA (NR2A-RNAi and NR2B-RNAi (Kim et al., 2005); plasmid coding for full length CaMKIIα (Sanhueza et al., 2011).

2.3 | Morphological analysis in vitro

GFP positive hippocampal or ventral spinal cord neurons were fixed in 4% paraformaldehyde (PFA) with 4% sucrose in PBS, mounted with Fluoromont-G and then visualized with epi-fluorescence (Nikon eclipse Ti, Tokyo, Japan) microscope, as previously described (Ampuero et al., 2017; Bustos et al., 2014; Henriquez et al., 2013; Sepulveda et al., 2010). To measure the number and length of individual dendrites, every branch segment arising from the soma was digitally marked from the origin of the branch to its termination using the plugin NeuronJ of the ImageJ software (NIH). Also, to measure the complexity of the dendritic arbor Sholl analysis was performed with ImageJ using a special plug-in designed by the laboratory of Dr. Anirvan Ghosh, UCSD (available at http://www-biology.ucsd.edu/labs/ghosh/software/index.html). Analysis was blinded to the experimental conditions.

2.4 | cLTP induction

To induce chemical LTP (cLTP) we used a protocol described by Fortin et al. (2010) with slight modifications. Briefly, cells were incubated for 2 hr with normal aCSF containing (in mM) 125 NaCl, 2.5 KCl, 2 $CaCl_2$, 1 $MgCl_2$, 5 HEPES; and 33 glucose; pH was adjusted to 7.3 using NaOH. Cells were rinsed with normal aCSF lacking Mg^{+2} and incubated for 3 min with aCSF containing glycine (200 µM), bicuculine (20 µM), and strychnine (3 µM) in the absence of Mg^{+2}. Cells were maintained for 3 or 33 min and fixed for immunostaining experiments.

2.5 | Immunofluorescence

Immunofluorescence assays were performed as previously described (Ampuero et al., 2017; Bustos et al., 2014). For immunofluorescence, cultures were rinsed twice in ice-cold PBS and fixed for 20 min in a freshly prepared solution of 4% PFA with 4% sucrose in PBS. Cells were rinsed three times in cold PBS and permeabilized for 5 min with 0.2% Triton X–100 in PBS. Next, cells were rinses in ice-cold PBS and incubated in 1% BSA plus 3% donkey serum in PBS for 30 min at 37°C, followed by an overnight incubation at 4°C with primary antibodies. Primary antibodies used were: CREB-P (1:200, rabbit polyclonal antibody, CAT #06519 Upstate); H3K27ac (1:2000, rabbit polyclonal antibody, CAT #ab4729 Abcam); Laminin B (1:500, goat polyclonal antibody, CAT #sc-6216, Santa Cruz). Cells were washed 3 times with PBS, then incubated with the corresponding Alexa-conjugated secondary antibodies (1:500, Thermo Fisher Scientific,) for 30 min at 37°C. Coverslips were mounted with Fluoromont-G (Electron Microscopy Sciences, Hatfield, PA) or DAPI-Prolong (Thermo Fisher Scientific, CAT#P36931). Samples were imaged by epi-fluorescent microscopy (Nikon eclipse Ti) or confocal laser microscopy (Olympus FV 1,000). Images were analyzed using NIH ImageJ software. Dual and triple immunofluorescent images were captured by multitracking imaging of each channel independently, to eliminate possible cross-talk between the different fluorophores.

2.6 | HSV injections

To express NR2ΔIN into hypoglossal motoneurons, we made use of herpex simplex virus (HSV) coding for HSV-GFP or HSV-GFP-NR2ΔIN under the IE 4/5 promoter. We used HSV-GFP viruses because the expression is robust and rapid (i.e., is initiated 2–3 hr post-injection) (Neve, Neve, Nestler, & Carlezon, 2005). Injections were performed as previously described (van Zundert et al., 2008). Briefly, high titer HSV was generated and injected (1 µl 7.5×10^7 U/ml) into one side of the tongue muscle of neonatal mice (P2-4) to retrogradely label hypoglossal motoneurons. Virus was slowly injected using a borosilicate glass electrode pipette held by a micromanipulator. At P6 animals were perfused using freshly prepared 4% PFA and sequential coronal slices were obtained from the brainstem. Slices were mounted into coverslips using Fluoromount G and images were acquired using confocal laser microscope (Olympus FV 1000) to reconstruct the z-axis.

Hippocampal neuron transductions were performed as previously described (Ampuero et al., 2017). Briefly, adult mice were anesthetized with saline (5 µl saline/gram body weight) containing 170 mg/kg ketamine plus 17 mg/kg xylazine. Stereotaxic injection was performed to target the granular layer of dentate gyrus of adult mice (2 month-old C57B6/SJL) following coordinates: ±1.5 mm lateral; −2 mm antero-posterior; −2.3 mm ventral from Bregma (Tashiro, Sandler, Toni, Zhao, & Gage, 2006). HSV-GFP or HSV-NR2AΔIN viruses were slowly injected using a borosilicate glass electrode pipette. 1.5 µl of 7.5×10^7 units/ml of virus was injected to determine viral efficiency. 0.5 µl of 3×10^7 U/ml was injected to quantify dendritic arbor and spine morphology 3 days after infection, animals were perfused using freshly prepared 4% PFA and sequential coronal slices were prepared from hippocampus. Slices were mounted into coverslips using Fluoromount G and images were acquired using confocal laser microscope (Olympus FV 1,000) to reconstruct the z-axis.

2.7 | Morphological analysis in vivo

Morphological analysis of hypoglossal motoneurons expressing GFP was performed as previously described (van Zundert et al., 2008). Briefly, animals were perfused with 4% PFA and brains were extracted immediately. Tissue was post-fixed overnight in 4% PFA and cryopreserved in 30% sucrose. To analyze infected HMs, 350 µm sequential sections through the entire brainstem were cut using a vibratome. Sections were permeabilized in 0.5% Triton X–100/PBS for 2 hr at RT and then blocked with 10% normal horse serum for 2 hr at RT. Sections were then incubated with a rabbit anti-GFP antibody coupled to Alexa-488 (CAT #A-21311, 1:400, Thermo Fisher Scientific). Slices were rinsed three times for 5 min in PBS and mounted using Fluoromount G. Images were acquired using confocal laser microscope (Olympus FV 1000) to reconstruct the z-axis. Morphological dendrite and spine analysis of hippocampal granule cells was performed as previously described (Ampuero et al., 2017). Three days post infection (see section HSV INJECTIONS) the animals were transcardially perfused with 4% PFA in PBS. Afterwards, the brain was removed immediately, post-fixed overnight and cryopreserved in sucrose gradient. The brains were cut serially in 40 µm sections on a cryostat (Leica, CM 152S, Germany). For morphometric analysis, at least 10 granular cells of the superior granular layer of the dentate gyrus of each experimental condition were selected, if they fulfilled the following criteria: (1) GFP positive signal along the entire dendritic field with high signal-to-noise ratio for GFP; (2) isolated from neighboring GFP infected granular cells; and (3) lack of truncated dendrites.

For the dendritic architecture of hippocampal granule cells, low-magnification images were acquired using a confocal laser scanning microscope Leica LSI Macro-Zoom with 63× oil objective (NA = 0.08, LWD Plan Apochromatic), excitation with solid state laser at 488 nm. 8-Bit TIFF images of 1,024 × 1,024 pixels were acquired with xy pixel size of 170 nm and 300 nm between z-sections. Forty to Fifty z-sections were acquired depending on the dendrite arbor of the neurons. Neurite Tracer of the Fiji software was used to measure the dendritic architecture and Sholl analysis plugins were used to evaluate the complexity of the dendritic arbor. Specifically, supragranular neurons located in the dentate gyrus were analyzed.

For spine analysis of hippocampal granule cells, high magnification images were acquired with an Olympus FluoView FV1000 confocal microscope with a 60× oil objective (NA = 1.3, C-Apochromat) and 4× digital zoom, excitation with a 488 nm diode laser (Omicron). 8-Bit TIFF images of 724 × 724 pixels were acquired with xy pixel size of 41 and 100 nm between z-sections. Images were deconvolved, segmented, and 3D reconstructions made.

2.8 | Statistical analyses

An ANOVA followed by the Dunnett's post-hoc test was used to evaluate statistic significance between experimental groups. Student's *t*-test was applied when two populations of responses were

examined. In all figures, error bars represent the SEM; $^{*}p \leq 0.05$, $^{**}p \leq 0.01$, $^{***}p \leq 0.001$.

3 | RESULTS

3.1 | TatCN21 differentially impacts dendritogenesis of cultured hippocampal neurons depending on the developmental stage

To test our hypothesis that the interaction between NR2B-NMDARs and CaMKII is necessary for dendritic growth, well-characterized culture systems, and tools were used. In the first set of experiments, we used the CaMKII inhibitor tatCN21, a peptide that disrupts the NR2B-NMDAR-CaMKII interaction and that can reverse LTP (Sanhueza et al., 2011; Vest, Davies, O'Leary, Port, & Bayer, 2007). Furthermore, unlike as seen with other fusion peptides such as ant in antCN27 (Buard et al., 2010), the fused tat sequence of tatCN21 allows membrane permeabilization without affecting calmodulin binding. Dendritogenesis was examined in primary hippocampal neurons of 7–12 days in vitro (DIV), because gain and loss-of function studies have shown that in these so-called intermediate neurons the expressed synaptic NR2B-rich receptors are required for dendrite formation and growth (Bustos et al., 2014; Sepulveda et al., 2010). To visualize the neuronal morphology, 7 DIV hippocampal neurons were transfected with a plasmid encoding a green fluorescent protein (GFP). Cultures were untreated (control) or treated once at 8 DIV with tatCN21 (5 μM; tatCN21) or scrambled tatCN21 (5 μM; tatCN21-SCR) as control peptide. At 12 DIV, neurons were fixed to assess the dendritic architecture of GFP-positive neurons. Intermediate hippocampal neurons treated with tatCN21 exhibited a strong reduction in dendritic architecture complexity relative to control or tatCN21-SCR neurons (Figure 1A). Higher magnification images of branches further showed that while filopodia-like protrusions are prominent in control neurons, these structures were largely absent in tatCN21 treated neurons (Figure 1A; insets).

Dendritic structure quantifications (Figure 1B) revealed that the number of secondary (left graph) and tertiary (middle graph) branches was robustly decreased in tatCN21 treated neurons, relative to control, or tatCN21-SCR treated neurons. The number of primary branches did not change under any of the tested conditions, and therefore, these measurements are not presented in this work. The summed length of all branches, termed total outgrowth, was also significantly decreased in tatCN21 treated neurons (Figure 1B; right graph). The finding that tatCN21-SCR treated hippocampal neurons displayed a morphology comparable to that of untreated control cells (Figure 1A and B) indicate that neither the tat peptide nor the fused peptide altered dendritic outgrowth in hippocampal cultures at the assessed concentrations. These results suggest that an interaction between CaMKII and NMDAR, likely through the NR2B subunit, is necessary for dendritic arborization and spine maturation in intermediate hippocampal neurons in vitro.

Our findings that the interaction between CaMKII and NMDAR is responsible for promoting dendritogenesis are in agreement with a previous study (Gaudillière et al., 2004), but are inconsistent with others (Ghiretti et al., 2013; Wu & Cline, 1998). To directly test if these contradictory results are due to the developmental stage of neurons, GFP-expressing hipocampal neurons were treated at 3 DIV with tatCN21 and fixed at 5 DIV. As controls, cells were untreated or incubated with tatCN21-SCR. In contrast to our finding in 12 DIV intermediate neurons, tatCN21 treatment caused the 5 DIV immature neurons to exhibit a more complex dendritic architecture (Figure 1C). Dendritic structure quantifications (Figure 1D) revealed significantly increases in secondary (left graph) and tertiary (middle graph) branches as well as in total branch outgrowth (right graph) relative to control or tatCN21-SCR treated neurons. Together, the results show that tatCN21 differentially impacts dendritogenesis of cultured hippocampal neurons depending on the developmental stage; in immature hippocampal neurons the NR2B-CaMKII interaction limits dendritogenesis, whereas in intermediate hippocampal neurons this interaction is required for dendritic outgrowth.

3.2 | Reducing the NR2B-CaMKII interaction with a mutant NR2B construct decreases dendritogenesis in intermediate hippocampal neurons

A series of experiments in intermediate hippocampal and spinal cord neurons were conducted to further test and strengthen the hypothesis that a specific interaction between the NR2B and CaMKII is needed for dendritogenesis. To first test the requirements of NR2B and CaMKII on dendritic growth in intermediate hippocampal neurons, 7 DIV cultures were transfected with GFP and either a construct encoding full-length CaMKIIα cDNA (CaMKII; Sanhueza et al., 2011) or a shRNA against NR2B (shRNA-NR2B; Kim et al., 2005; Sepulveda et al., 2010). At 12 DIV, cultures were fixed, and GFP-positive neurons were imaged to analyze their neuronal architecture (Figure 2). Intermediate hippocampal neurons over-expressing CaMKII showed increased dendritic arbor complexity (Figure 2A), giving arise to significantly more secondary (Figure 2B) and tertiary (Figure 2C) processes, as well as increased total branch outgrowth (Figure 2D) relative to the control. In agreement with our previous study (Sepulveda et al., 2010), expression of shRNA-NR2B reduced all of these parameters in intermediate neurons (Figure 2A–D). Fluorescent microscopy images also showed that neurons expressing both CaMKII and shRNA-NR2B displayed a strongly reduced dendritic architecture comparable to that of neurons expressing shRNA-NR2B alone (Figure 2A). Quantifications further revealed that neurons exhibited significantly reduced numbers of secondary (Figure 2B) and tertiary (Figure 2B) branches, as well as total branch outgrowth (Figure 2D) relative to the control. These results support the role of the NR2B subunit in intermediate hippocampal neuron dendritogenesis (Bustos et al., 2014; Sepulveda et al., 2010). Additionally, the finding that CaMKII over-expression in NR2B-silenced cells failed to rescue the branching complexity indicates that the NR2B-CaMKII interaction, and not just the

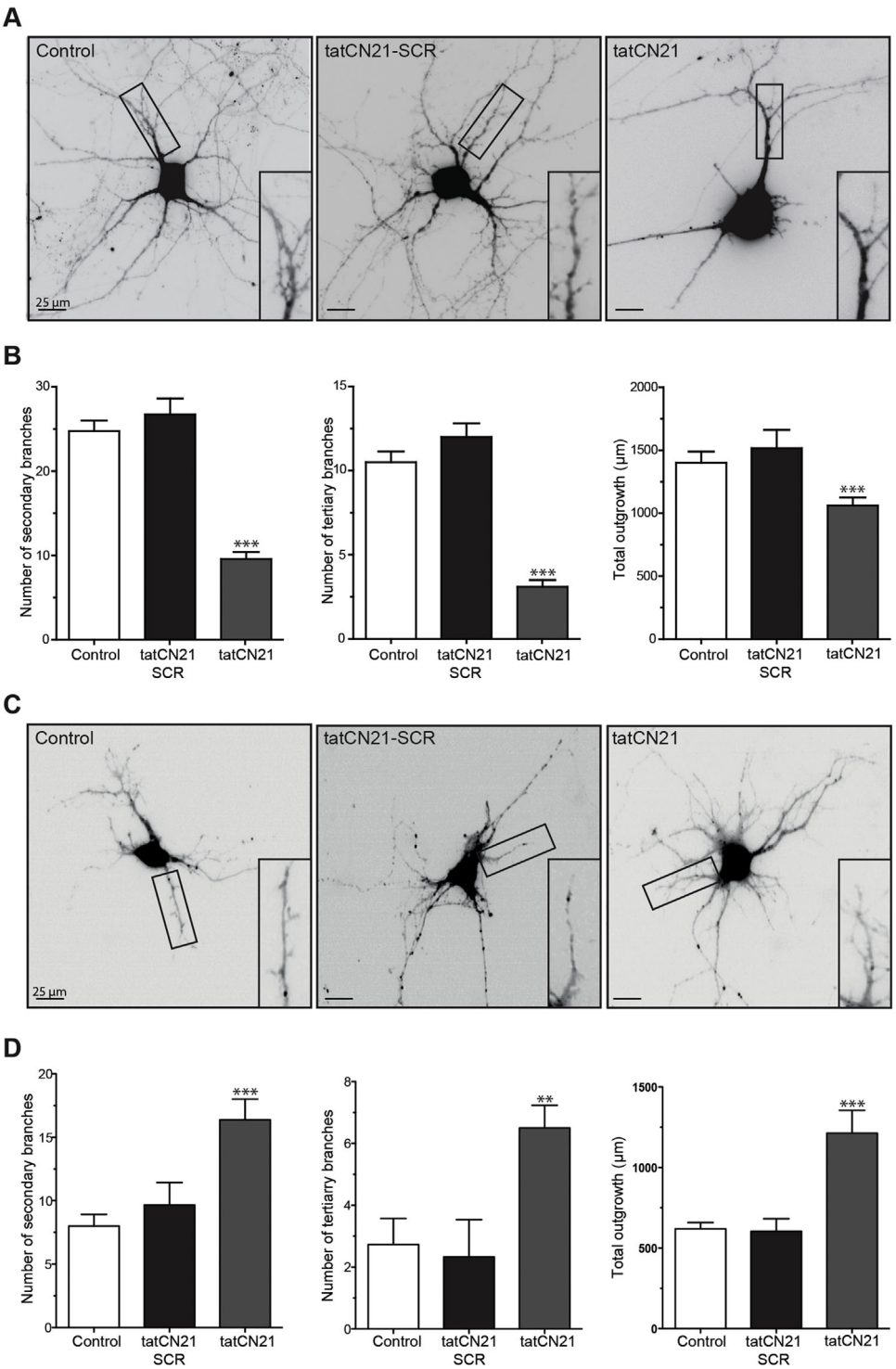

FIGURE 1 TatCN21 differentially impacts dendritogenesis of cultured hippocampal neurons depending on the developmental stage. Uncoupling of the NMDAR-CaMKII interaction with bath-applied tat-fused CN21 peptide (tatCN21) (A and B) decreases dendritogenesis of maturing neurons but (C and D) increases dendritic outgrowth of immature neurons. At (A and B) 7 or (C and D) 2 days in vitro (DIV) hippocampal neurons were transfected with GFP. The following day, cultures were left untreated (control) or incubated with either control scrambled peptide tatCN21 (tatCN21-SCR) or tatCN21 (tatCN21). At (A and B) 12 DIV or (C and D) 5 DIV, cultures were fixed with 4% PFA; images were acquired on a fluorescent microscope, and the architecture of the transduced neurons was analyzed. (A and C) Representative contrast-enhanced images of (left) control, (middle) tatCN21-SCR, and (right) tatCN21 neurons. Insets: amplification of boxed areas. (B and D) Quantification (i.e, average number) of (left) secondary and (middle) tertiary branches and of (right) total as indicated. For each condition, at least 10 neurons obtained from three independent experiments were analyzed. Values represent mean ± S.E.M. ***$p \leq 0.001$ relative to control conditions. One-way ANOVA followed by Dunnett's post-hoc test

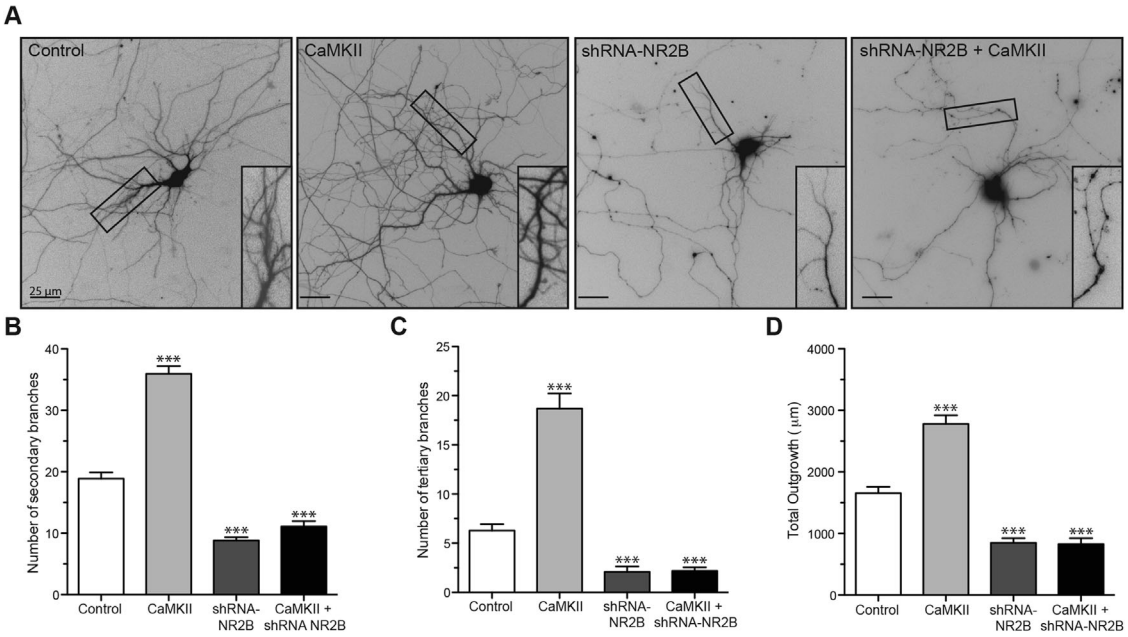

FIGURE 2 Knock-down of NR2B-NMDARs decreases CaMKII-dependent dendritogenesis of maturing hippocampal neurons in vitro. Dendritogenesis of maturing hippocampal neurons (12 DIV) is mediated by NR2B-NMDARs and CaMKII. Hippocampal neurons (7 DIV) were transfected with either GFP (control), GFP + CaMKII (CaMKII), GFP + shRNA-NR2B (shRNA-NR2B), or GFP + shRNA-NR2B + CaMKII (shRNA-NR2B + CaMKII). Transduced neuron morphology was analyzed at 12 DIV. (A) Representative contrast-enhanced images of control and treated neurons as indicated. Insets: amplification of boxed areas. (B–D) Quantification (i.e, average number) of (B) secondary and (C) tertiary branches and of (D) total outgrowth as indicated. For each condition, at least 10 neurons obtained from three independent experiments were analyzed. Values represent mean ± S.E.M. ***$p \leq 0.001$ relative to control conditions. One-way ANOVA followed by Dunnett's post-hoc test

presence of CaMKII, is required to induce changes in dendritic growth.

To specifically test if the interaction between endogenous CaMKII and NR2B-NMDARs is necessary to induce dendritic outgrowth in intermediate hippocampal neurons in vitro, we made use of the NR2B mutant NR2B-RS/QD. This construct contains a double mutation in the C-terminal tail (Arg1300 and Ser1303 mutated to Gln and Asp) that leads to a strongly diminished binding to active CaMKII (Barria & Malinow, 2005; Gambrill & Barria, 2011; Mayadevi et al., 2002). In intermediate hippocampal neurons, NMDARs do not only exist as di-heteromers (e.g., NR1/NR2A or NR1/NR2B), but also as tri-heteromers (e.g., NR1/NR2A/NR2B) (Al-Hallaq et al., 2007; 2003; Sans et al., 2000; Sheng, Cummings, Roldan, Jan, & Jan, 1994; van Zundert et al., 2004). Given that tri-heteromeric receptors complicate the interpretation of NR2B-RS/QD-related results (see Discussion), we opted to make use of intermediate spinal cord neurons that lack NR2 subunits (but not NR1) and therefore are natural NR2 knock-out cells (Bustos et al., 2014; Mi et al., 2004; Sepulveda et al., 2010). These spinal cord neurons express functional AMPARs, $GABA_A$Rs, and GlyRs at the synapses but lack functional NMDARs, which can be recovered by the expression of the NR2A or NR2B subunits to form synaptic NR2A- or NR2B-NMDARs, respectively (Sepulveda et al., 2010). Spinal cord cultures at 4 DIV were transfected with GFP alone (control), GFP plus the NR2B-RS/QD construct (NR2B-RS/QD), or GFP plus the NR2B construct (NR2B) as a positive control. At 10 DIV, cultures were fixed, and GFP-positive neurons were imaged to analyze their neuronal architecture (Figure 3). In agreement with our previous studies (Bustos et al., 2014; Sepulveda et al., 2010), spinal cord neurons expressing NR2B displayed a more complex dendritic architecture (Figure 3A), with significantly more secondary (Figure 3B) and tertiary (Figure 3C) processes, as well as increased total branch outgrowth (Figure 3D) relative to control neurons. In contrast, fluorescent images and quantifications show that spinal cord neurons expressing NR2B-RS/QD displayed a strong reduction in dendritic architecture complexity with significantly decreased branch number and total outgrowth (Figure 3A–D) compared to control and NR2B-expressing neurons. Together, the use of two different neuronal culture systems and several molecular tools, including the tatCN21 peptide, and the CaMKII, shRNA-NR2B, and NR2B-RS/QD constructs, provide evidence that the coupling of NR2B-NMDARs to CaMKII is necessary for dendritic growth in intermediate neurons.

3.3 | Mature hippocampal neurons in vitro expressing NR2AΔIN, a mutant NR2A construct with increased interaction to CaMKII, display dendritic outgrowth

Next, we tested our hypothesis that dendritic arbor stability in mature neurons is, at least in part, regulated by the dominant synaptic NR2A expression and a limited interaction of this subunit with CaMKII. For this, the previously characterized mutant NR2A subunit construct NR2AΔIN was used. This construct contains a double amino acid deletion (Ile1286 and Asn1287) in the C-terminal tail that leads to a significant increased interaction with active CaMKII (Barria & Malinow,

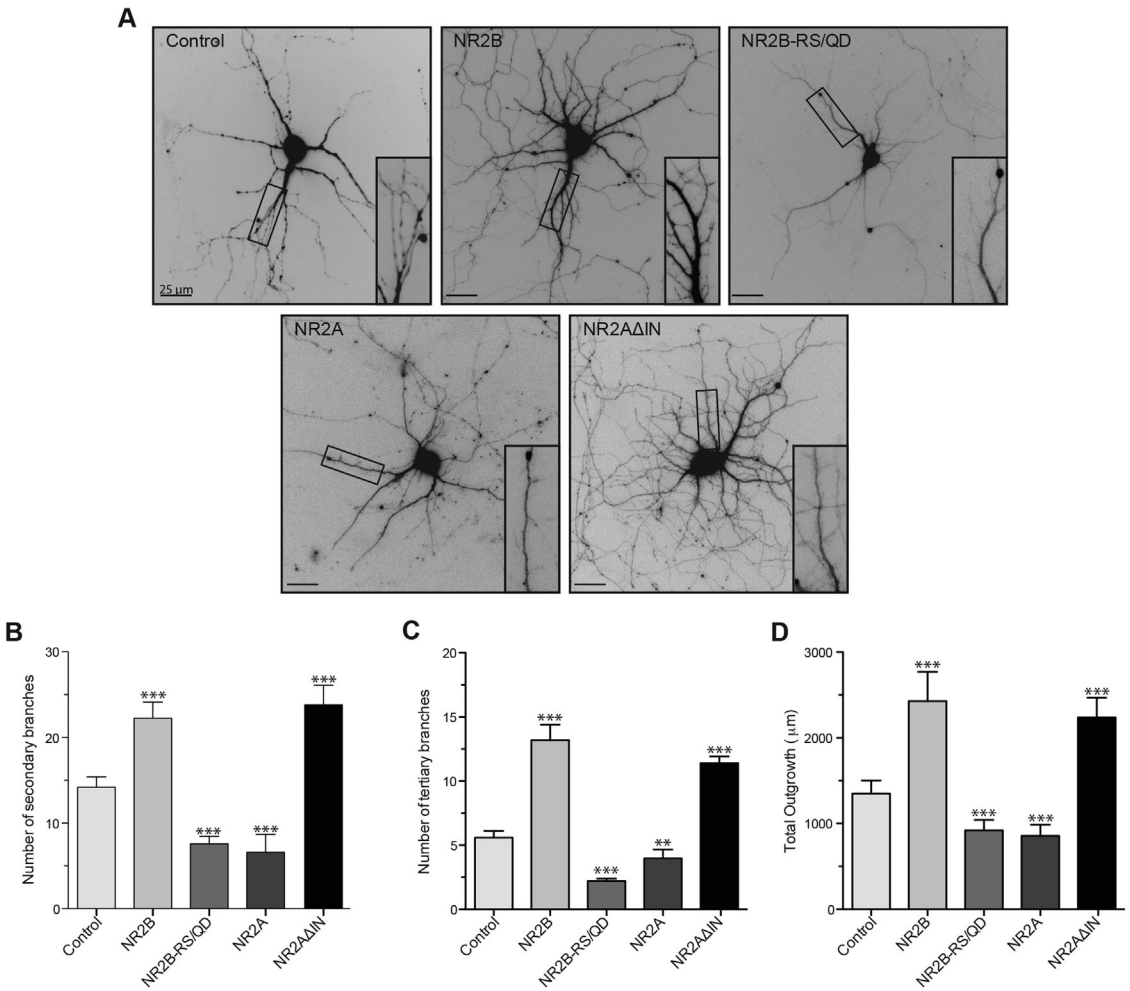

FIGURE 3 Dendritogenesis of cultured spinal cord neurons is increased when transducing NR2B or NR2AΔIN. Dendritogenesis of spinal cord neurons (NR2 knock-out cells) increases when transducing wild-type NR2B-NMDARs (NR2B) or mutant NR2A-NMDARs (NR2AΔIN) constructs with known endogenous CaMKII interactions. Contrary, dendritogenesis is decreased when transducing wild-type NR2A-NMDARs (NR2A) or mutant NR2B-NMDARs (NR2BRS/QD), constructs with limited endogenous CaMKII interactions. Spinal cord neurons (4 DIV) transfected with either GFP (control), GFP + NR2B (NR2B), GFP + NR2B-RS/QD (NR2B-RS/QD, with reduced NR2B-CaMKII interaction), GFP + NR2A (NR2A), or GFP + NR2AΔIN (NR2AΔIN, with increased NR2A-CaMKII interaction). Cultures (10 DIV) were fixed and the transduced neuron architecture was analyzed. (A) Representative contrast-enhanced images of control and treated neurons as indicated. Insets: amplification of boxed areas. (B–D) Quantification (i.e., average number) of (B) secondary and (C) tertiary branches and of (D) total outgrowth as indicated. For each condition, at least 10 neurons obtained from three independent experiments were analyzed. Values represent mean ± S.E.M. $^{**}p \leq 0.01$ and $^{***}p \leq 0.001$ relative to control conditions. One-way ANOVA followed by Dunnett's post-hoc test

2005; Gambrill & Barria, 2011; Mayadevi et al., 2002). We first tested the role of NR2AΔIN on dendritogenesis in NR2 knock-out spinal cord neurons, as described above. Thus, 4 DIV spinal cord cultures were transfected with GFP alone (control), GFP plus NR2AΔIN (NR2AΔIN), or GFP plus NR2A (NR2A) as a positive control. At 10 DIV, cultures were fixed, and GFP-positive neurons were imaged to analyze their neuronal architecture (Figure 3). In agreement with our previous studies (Bustos et al., 2014; Sepulveda et al., 2010) fluorescent images and quantifications revealed that those spinal cord neurons expressing NR2A displayed a much less complex dendritic architecture relative to control cells (Figure 3A), with a significantly reduced number of secondary (Figure 3B) and tertiary (Figure 3C) processes, as well as a decreased total branch outgrowth (Figure 3D). In contrast, spinal cord neurons transduced with NR2AΔIN exhibited a more complex dendritic architecture with significantly increased branches and total outgrowth compared to control and NR2A-expressing neurons (Figure 3A–D).

Having found that NR2AΔIN increased dendritic outgrowth in spinal cord neurons, we next tested if this NR2A mutant construct was able to reactivate dendritogenesis in mature hippocampal neurons in vitro. For this, we analyzed 20–21 DIV mature hippocampal neurons, since they predominantly express synaptic NR2A-NMDARs and display a stable dendritic architecture (Bustos et al., 2014; Sepulveda et al., 2010). Hippocampal cultures were transfected at 16 DIV with GFP alone, GFP plus NR2AΔIN (NR2AΔIN), or GFP plus NR2A (NR2A). At 21 DIV, cultures were fixed, and GFP-positive neurons were imaged to analyze the neuronal architecture (Figure 4). Notably, mature hippocampal neurons expressing NR2AΔIN displayed a much more

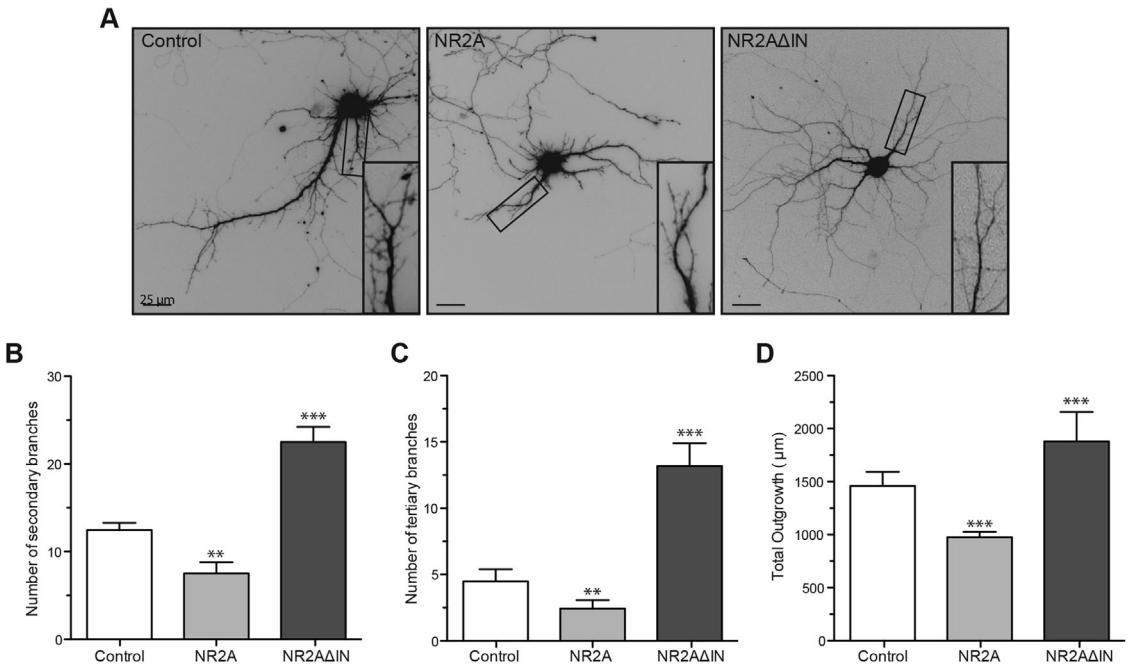

FIGURE 4 NR2AΔIN increases dendritogenesis of mature hippocampal neurons in vitro. Mature hippocampal neurons transducing NR2AΔIN display robust dendritogenesis. Hippocampal neurons (16 DIV) were transfected with either GFP (control), GFP plus NR2A (NR2A), or GFP plus NR2AΔIN (NR2AΔIN). Transduced neuron morphology was analyzed at 21 DIV. (A) Representative contrast-enhanced images of control and treated neurons as indicated. Insets: amplification of boxed areas. (B–E) Quantification (i.e., averaged number) of (B) secondary and (C) tertiary branches and of (D) total outgrowth as indicated. For each condition, at least 10 neurons obtained from three independent experiments were analyzed. Values represent mean ± S.E.M. $^{**}p \leq 0.01$ and $^{***}p \leq 0.001$ relative to control conditions. One-way ANOVA followed by Dunnett's post-hoc test

complex dendritic architecture (Figure 4A) with significantly decreased branches and total outgrowth (Figure 4B–D) compared to control and NR2A-expressing neurons.

3.4 | Dendrites of NR2AΔIN-transduced hypoglossal motoneurons in vivo cross less the midline compared to control neurons

Since NR2AΔIN reactivated dendritogenesis in spinal cord and hippocampal neurons in vitro, we sought to test if this construct was able to impact dendritogenesis in vivo in hypoglossal motoneurons (Figure 5) and hippocampal neurons (Figure 6). For transduction, we generated viral herpes simplex virus (HSV) particles expressing enhanced GFP alone (control, HSV-GFP) or GFP together with NR2AΔIN (HSV-NR2AΔIN). Expression of NR2AΔIN by HSV infection is controlled by an IE 4/5 promoter, while GFP expression to visualize complete dendritic arbor is controlled by a CMV promoter. We chose to examine hypoglossal motoneurons, because these neurons display a dendritic architecture that is robustly and stereotypically altered during early postnatal maturation. Specifically, retrograde labeling has revealed that while these motoneurons express a complex dendritic architecture with dendrites crossing the brainstem midline at P6, the contralateral-positioned dendrites rapidly retract during the next 3 days of postnatal development (Nunez-Abades & Cameron, 1995; van Zundert et al., 2008). To transduce hypoglossal motoneurons with GFP or GFP plus NR2AΔIN, P2-4 mouse littermates were injected with HSV-GFP (control) or HSV-NR2AΔIN into the tongue muscle, respectively (Figure 5A). At P6, animals were sacrificed and fixed, and coronal brainstem slices prepared. In agreement with our previous studies (van Zundert et al., 2008), confocal fluorescent images and quantifications revealed that dendrites of control hypoglossal motoneurons cross the midline at P6 (Figure 5B and C). In contrast, those neurons infected with HSV-NR2AΔIN showed significantly fewer dendrites crossing the midline compared to control neurons (Figure 5B and C). These results indicate that increased NR2A-CaMKII interaction leads to increased dendritic maturation of hypoglossal motoneurons in vivo.

3.5 | NR2AΔIN reactivates dendritogenesis in mature hippocampal neurons in vivo

Next, we tested if NR2AΔIN could reactivate dendritogenesis in mature hippocampal neurons in vivo. The dendritic arbors of hippocampal excitatory neurons reach their mature size by P18-21 and remain largely stable over the next 3.5–4 months (Burt, 1980; Koleske, 2013; Sfakianos et al., 2007). Considering this, 2-months-old mature hippocampal neurons were used to examine if NR2AΔIN increased dendritic outgrowth. To transduce adult hippocampal neurons in vivo, 2-months-old mice were stereotaxically injected with HSV particles in the dentate gyrus. Three days later, when HSV-containing genes are maximally expressed (Barrot et al., 2002; and data not shown), the animals were sacrificed and perfused with 4% PFA.

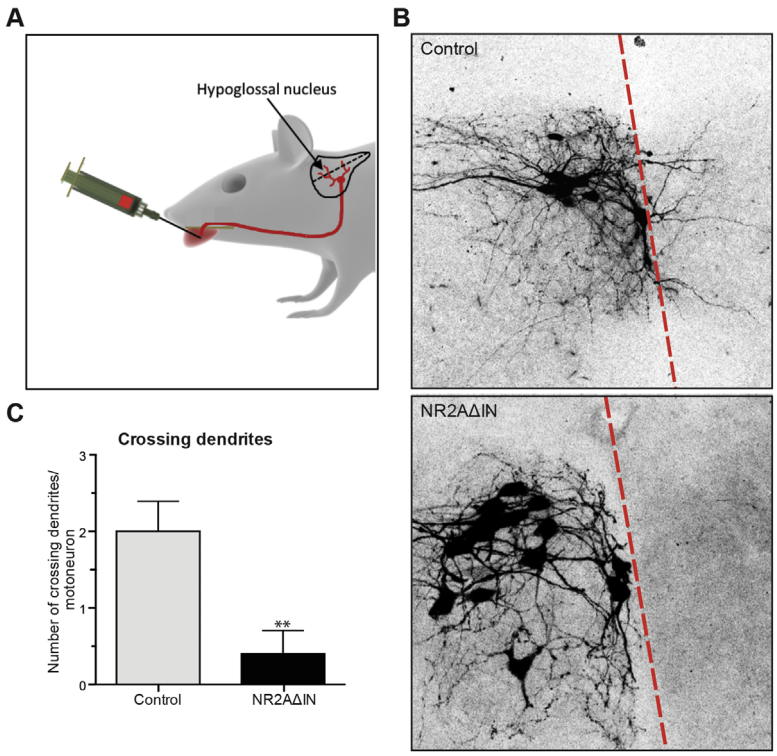

FIGURE 5 Viral-mediated expression of NR2AΔIN in vivo increases dendrite remodeling of P6 hypoglossal motoneurons. Hypoglossal motoneurons infected with herpes simplex virus (HSV) particles expressing NR2AΔIN display robust changes in dendritic remodeling. (A). Schematic of the experiment. HSV particles expressing GFP alone (HSV-GFP) or GFP plus NR2A-ΔIN (HSV-NR2AΔIN) were generated and injected (1 µl 7.5×10^7 U/ml) into the one side of tongue muscle of neonatal mice (P2-4) to retrogradely label hypoglossal motoneurons. At P6, animals were perfused (4% PFA) and coronal slices (350 µm) were prepared from the brainstem. (B) Confocal magnification image (20×) shows that tongue-injected HSV specifically transduce ipsilateral hypoglossal motoneurons (nXII). In animals transducing NR2AΔIN fewer dendrites crossed the midline (dashed line) at P6 compared to control condition. (C) Quantification of averaged number branches that cross the hypoglossal midline. For each condition, at least 10 neurons obtained from three independent experiments were analyzed. Values represent mean ± S.E.M. $^*p \leq 0.05$ relative to control conditions (Studenťs *t*-test)

Coronal hippocampi slices were prepared to analyze the neuronal architecture of GFP-positive neurons (Figure 6A and B); dendritic processes (Figure 6C and D) as well as dendritic spine density (Figure 6E and F) were assessed.

Low magnification confocal images showed that high HSV-GFP titer injections efficiently transduced the different layers of the dentate gyrus, including the supragranular, infragranular, and hilus layers. For morphological analyses, low HSV-GFP and HSV-NR2AΔIN titers were injected, and only granular cells were selected. Granular cell morphology is well-characterized (Ampuero et al., 2017; Jain et al., 2012; Zhao, Teng, Summers, Ming, & Gage, 2006) with localization of the cell body in the supragranular layer and dendritic branch projections toward the molecular layers (Figure 6A and B). Under control conditions, the GFP-positive granular cells displayed a dendritic arbor with several secondary processes emerging from the primary dendritic process, as previously described (Ampuero et al., 2017; Gonçalves et al., 2016; Zhao et al., 2006). Interestingly, adult granular neurons transducing NR2AΔIN displayed a more complex dendritic arbor (Figure 6B) with significantly increased total dendritic length (Figure 6C) relative to control neurons. Sholl analyses further revealed that, relative to control neurons, NR2AΔIN-expressing granular neurons exhibited more dendritic branches located >50 µm from the soma (Figure 6D). These results are consistent with our present finding that NR2AΔIN induced dendritogenesis in mature hippocampal neurons in vitro (Figure 4).

To determine the impact of NR2AΔIN on spine density, we analyzed dendritic protrusions on second order branches located in the medium molecular layer of selected granular neurons. Consistent with previous studies (Ampuero et al., 2017; Jain et al., 2012), mature granular neurons were decorated with substantial quantities of dendritic protrusions, including mushroom, stubby and thin spines, with few filopodia (Figure 6E). In contrast, NR2AΔIN-transducing granular cells displayed dendrites with much fewer dendritic protrusions, particularly in regards to mushroom spines, leading to significantly decreased spine density (Figure 6E and F). Dendritic branch diameter quantification further revealed that NR2AΔIN significantly reduced this parameter relative to control cells (Figure 6G). Altogether, transduction of the NR2AΔIN construct in mature granular neurons in vivo enhanced dendrite arbor complexity and reduced the diameter of the dendritic branches, which were decorated with less mature spines. These results suggest that increased coupling of NR2A-NMDARs to endogenous CaMKII induces structural plasticity in adult hippocampal neurons, leading to a more complex and immature-like dendritic architecture.

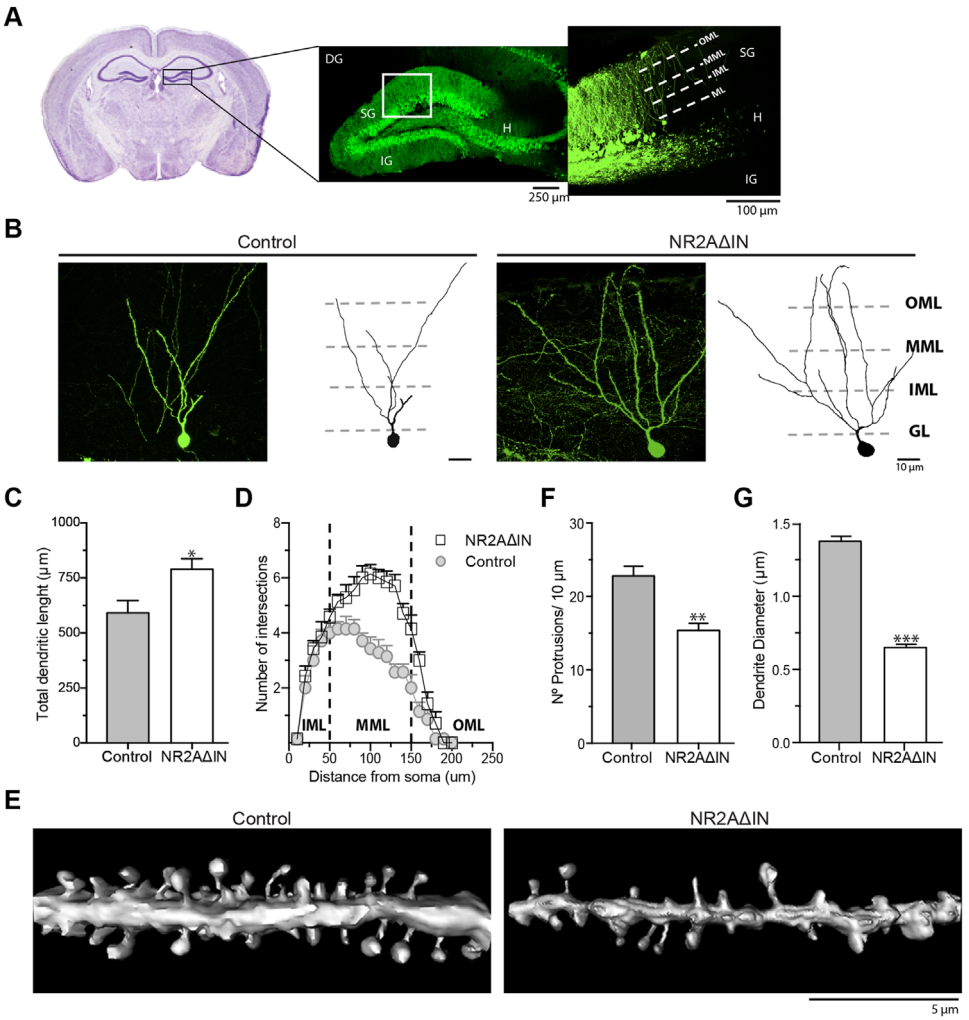

FIGURE 6 Viral-mediated expression of NR2AΔIN in vivo increases dendritogenesis and reduces spine density of dentate gyrus hippocampal neurons. Dendritogenesis is increased in mature hippocampal transducing NR2AΔIN. HSV particles harboring GFP (HSV-GFP) or GFP plus NR2AΔIN (HSV-NR2AΔIN) were stereotaxically injected in adult mice (2-months-old) into the dentate gyrus (DG): (A) 1.5 µl of 7.5×10^7 U/ml for viral efficiency and (B–G) 0.5 µl of 3×10^7 U/ml for dendritic and spine morphology. Three days post-injection, animals were perfused (4% PFA) and coronal slices were prepared from hippocampi. (A) Low magnification images (10×) show that HSV-GFP injections efficiently transduce the different DG layers, including the supragranular (SG), infragranular (IG) and hilus (H) layer. In SG layer, the inner, medium and outer molecular layer (IML, MML, and OML, respectively) are indicated. Granular cells in SG were selected for morphological analyses. (B–D) Hippocampal granular neurons transduced with NR2AΔIN display a more complex dendritic arbor compared to control neurons. (B) Representative confocal images (60×) show 2D reconstructions from isolated neurons transducing HSV-GFP (left) or NR2AΔIN (right). Quantification of the (C) averaged total dendritic outgrowth and (D) Sholl analysis. For each condition, at least 10 neurons, obtained from three independent experiments, were analyzed. Figures show Means ± S.E.M. $^*p \leq 0.05$ (*t*-test). (E and F) Spine density is decreased in hippocampal granular neurons transduced with NR2AΔIN. (E) Representative confocal images (60× and 4× digital zoom; 100 nm optical sections; stacked 6–10 µm) of GFP-positive DG neurons were deconvoluted to generate 3D reconstructions with ImageJ Fiji software. Quantification of (F) spine density and (G) average dendrite diameter. For each condition, at least 20 dendrite segments of the MML, obtained from three independent experiments, were analyzed. Means ± S.E.M. $^{**}p \leq 0.01$ and $^{***}p \leq 0.001$ relative to control conditions (Students *t*-test)

3.6 | Activation of NR2AΔIN-NMDARs in mature hippocampal neurons by cLTP does not produce a concomitant increase in CREB-P and H3K27ac

Finally, we wanted to gain insights into the underlying signaling and epigenetic mechanisms that regulate NMDAR-mediated dendritogenesis at the cellular level by using immunofluorescence staining. For the synapse-to-nucleus signaling pathway, we focused on phosphorylated CREB. This kinase is phosphorylated and hence activated by many serine/threonine kinases, including CaMKII, which in turn is activated by calcium influx through voltage-sensitive calcium channels and synaptic NMDARs (Bito, Deisseroth, & Tsien, 1996; Greer & Greenberg, 2008). We first validated if the stimulation of synaptic NMDARs in mature hippocampal cultures (20 DIV) was able to activate CREB, as detected by the phosphorylation of serine 133 (CREB-P). To activate synaptic NMDARs, we used a chemical LTP (cLTP) protocol

(Fortin et al., 2010), and tested CREB-P at 3 and 33 min post-stimulation (Figure 7A). As with electrical stimuli (Bito et al., 1996), we found in hippocampal neurons that cLTP robustly and transiently increased nuclear CREB-P levels, with highest immunoreactivity recorded at 3 min post-stimulation (data not shown). Next, neurons (15 DIV) were transfected with GFP (GFP) or GFP plus NR2AΔIN (NR2AΔIN) using Magnetofection. At 20 DIV, cLTP was induced and CREB-P immunostaining performed (Figure 7A). Compared to untransfected control neurons, NR2AΔIN-expressing neurons showed higher nuclear CREB-P levels 3 min after the cLTP stimulus (Figure 7B). These results were expected as the NR2AΔIN construct enhances the coupling of NR2AΔIN to endogenous CaMKII (Barria & Malinow, 2005).

Activated CREB, through stimulated synaptic NMDARs or voltage-sensitive calcium channels, initiates a transcriptional program of plasticity-associated genes that drives spine maturation (West et al., 2001; West & Greenberg, 2011). Mechanistically, CREB-P recruits CREB-binding protein (CBP) to promoters, either alone or with the highly homologous co-activator p300 (Hardingham, Chawla, Cruzalegui, & Bading, 1999). The CBP/p300 proteins mediate the acetylation of lysine 27 of histone H3 (H3K27ac), a known activation-associated histone mark that is implicated in the recruitment of RNA polymerase cofactors and hence induces transcription (Bannister & Kouzarides, 2011). Here we wanted to determine if cLTP-mediated CREB-P produces a concomitant increase in global H3K27ac levels. To visualize nuclear H3K27ac staining, co-localization assays were performed with nuclear marker DAPI and Laminin-B. We found that cLTP increased nuclear H3K27ac levels at 33 min post-stimulation in untransfected and GFP-transfected neurons (Figure 7C). Surprisingly, relative to untransfected control neurons, NR2AΔIN expressing mature hippocampal neurons displayed lower nuclear H3K27ac levels at both 3 and 33 min post-stimulation (Figure 7D). Together, our data show that unlike control neurons, cLTP-stimulated mature hippocampal neurons expressing NR2AΔIN increases CREB-P levels that do not correlate with higher global H3K27ac levels.

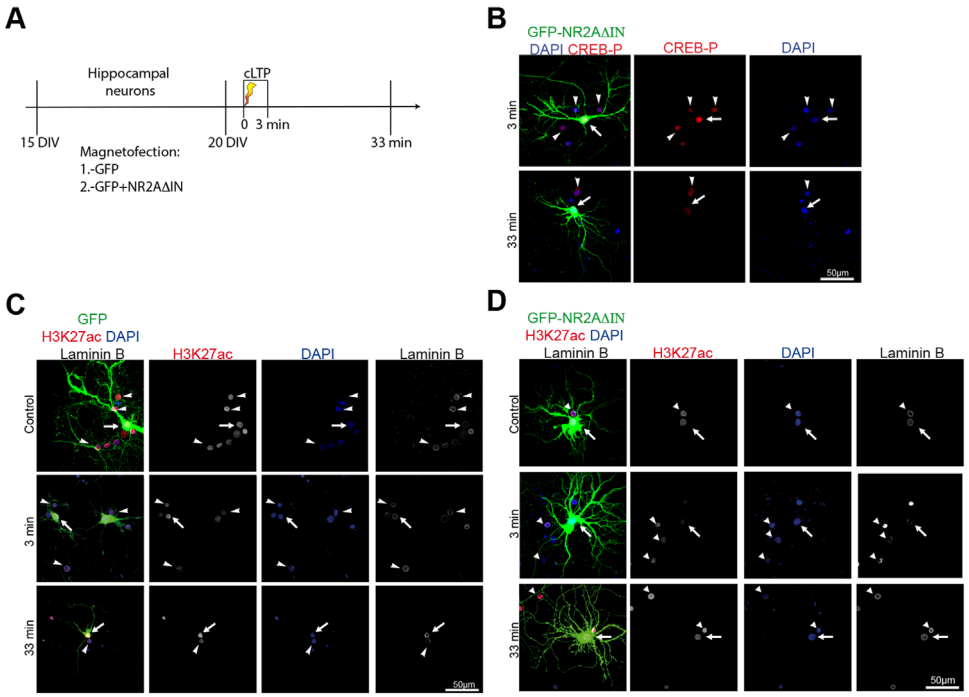

FIGURE 7 cLTP does not produce a concomitant increase in CREB-P and H3K27ac in mature hippocampal neurons expressing NR2AΔIN. (A) Schematic of the experiment. Hippocampal cultures (15 DIV) were transfected with GFP (GFP) or GFP plus the NR2AΔIN construct (NR2AΔIN) using Magnetofection. At 20 DIV, cultures were incubated with aCSF containing Mg^{+2} for 2 hr, washed with ACSF lacking Mg^{+2}, and then incubated for 3 min with aCSF containing glycine (200 μM), bicuculine (20 μM) and strychnine (3 μM) in the absence of Mg^{+2}. After induction of chemical LTP (cLTP), cultures were maintained for 3 or 33 min and fixed, followed by immunostaining to detect CREB-P or H3K27ac. (B) Compared to untransfected control neurons, NR2AΔIN-transducing neurons showed higher nuclear CREB-P levels 3 min after the cLTP stimulus. Representative confocal image of a NR2AΔIN-transfected neurons (green) immunostained to detect CREB-P (red) and mounted with DNA marker DAPI (blue). Z-maximal projections of at least 5–7 focal planes of 1 μm are shown. (C and D) Increased CREB-P levels in control and GFP-transducing neurons, but not in NR2AΔIN-transducing neurons, is correlated with higher global H3K27ac levels. Neurons were transfected with GFP alone (C) or with GFP and NR2AΔIN (D), and induced with cLTP as described above. At 3 or 33 min after cLTP induction, cells were fixed, and immunostained to detect H3K27ac. Representative confocal images showing transfected neurons (green) expressing GFP alone (C) or GFP plus NR2AΔIN (D), and immunostaining for H3K27ac (red and grey scales for clarity) and Laminin B (white), and DAPI stain (blue) are also shown. Transfected and untransfected neurons are indicated by arrows and arrowheads, respectively. Note that H3K27ac levels in GFP-transfected neurons were similar to untransfected neurons, indicating that the transfection assay did not induce adverse effects on this signaling pathway. Also note that nuclear H3K27ac levels in NR2AΔIN-transducing neurons are lower compared to surrounding untransfected control neurons. Similar results were found in two other independent cultures. Scale bar 50 μm

4 | DISCUSSION

In this study, we investigated if a direct interaction between specific NMDAR subunits and CaMKII regulates structural plasticity. Using diverse in vitro and in vivo neuronal models, the main three findings were as followed: (1) NR2B-NMDAR-CaMKII complexes limit dendritic outgrowth in immature neurons but promote dendritogenesis in intermediate neurons; (2) the NMDARs to CaMKII association induces dendritogenesis in intermediate neurons, independent of the presence of either the NR2A, or NR2B NMDAR subunits; (3) dendritogenesis can be reactivated in the adult brain by enhancing the coupling of NR2A-NMDARs to endogenous CaMKII. Additionally, we sought to gain insights into the membrane-to-nucleus signals and epigenetic mechanisms that underlie NMDAR-CaMKII-mediated dendritogenesis. Our data indicate that activation of the NMDAR/CaMKII/ERK-P/CREB-P signaling axis in mature control neurons, unlike NR2AΔIN expressing neurons, is correlated with global increases in H3K27ac.

Diverse gain-and-loss-of-function approaches in several experimental systems imply that CaMKII regulates dendritic outgrowth, but results are inconsistent (Gaudillière, Konishi, la Iglesia de, Yao, & Bonni, 2004; Ghiretti et al., 2013; Wu & Cline, 1998). Particularly, RNAi-mediated CaMKII knock-down assays in cultured cerebellum neurons derived from postnatal rats indicate that CaMKII promotes arbor complexity (Gaudillière et al., 2004). In contrast, conclusions drawn from overexpression of a dominant-negative CaMKII form in *Xenopus laevis* tadpole tectal neurons (Wu & Cline, 1998) and from the treatment of immature embryonically-derived cultured hippocampal neurons (5 DIV) with the CaMKII-specific peptide inhibitor CaMKIIN (Ghiretti et al., 2013) indicate that CaMKII is a negative dendritic outgrowth regulator. In agreement with Gaudillière et al. (2004), we found that tatCN21 peptide application increased dendritic outgrowth and branching in embryonically-derived immature hippocampal cultures (5 DIV). Consistent with the studies by Wu and Cline (1998) and Ghiretti et al. (2013), we found that tatCN21 and NR2B-RS/QD impaired dendritogenesis in intermediate hippocampal neurons (12 DIV) and spinal cord neurons (12 DIV), while overexpression of CaMKII increased dendritogenesis in both these neurons. Our results suggest that prior contradictory results (Gaudillière et al., 2004; Ghiretti et al., 2013; Wu & Cline, 1998) might be explained, at least in part, by the different developmental neuronal stages used in each study. Therefore, our data indicate that CaMKII activity limits dendritogenesis in immature neurons but promotes dendritic branching and outgrowth in intermediate neurons.

To determine the role of NR2B-NMDARs in CaMKII-mediated dendritogenesis, we used gain- (CaMKII cDNA) and loss-of-function (shRNA-NR2B) constructs, as well as the NR2B-RS/QD construct and the tatCN21 peptide, both known to specifically interfere in the recruitment and interaction of CaMKII to the NR2B C-terminal domain (Barria & Malinow, 2005; Gambrill & Barria, 2011; Sanhueza et al., 2011). We found that shRNA-NR2B, NR2B-RS/QD, and tatCN21 impaired dendritic outgrowth and branching in intermediate hippocampal neurons. Additionally, the CaMKII overexpression in intermediate hippocampal neurons was sufficient to strongly enhance dendritogenesis, an effect that was lost when endogenous NR2B-NMDARs expression was reduced by shRNA. These results indicate that the direct intreaction between NR2B-NMDARs and CaMKII is necessary to induce dendritogenesis in intermediate hippocampal neurons.

We studied intermediate hippocampal cultures (12 DIV) that exhibit strong NR2B-NMDAR-dependent dendritic growth (Bustos et al., 2014), Furthermore, the role of synaptic CaMKII expression in LTP and synaptic plasticity is well studied in these cultures (Dupuis et al., 2014; Opazo et al., 2010; Sanz-Clemente, Gray, Ogilvie, Nicoll, & Roche, 2013). However, a disadvantage is that intermediate hippocampal neurons abundantly express tri-heteromeric NMDARs (Tovar, McGinley, & Westbrook, 2013), possibly affecting the result interpretation. More specifically, synaptic NR1, NR2A, and NR2B subunits can exist in vivo and in vitro not only as di-heteromers (e.g., NR1/NR2A or NR1/NR2B), but also as tri-heteromers (e.g., NR1/NR2A/NR2B) (Al-Hallaq et al., 2007; Dunah & Standaert, 2003; Sans et al., 2000; Sheng et al., 1994; Tovar et al., 2013; van Zundert et al., 2004). The presence of tri-heteromers, especially in intermediate neurons, complicates dissecting out the contribution of individual NMDAR subunits in neuronal plasticity processes, and in this study, in specific interactions with CaMKII. To circumvent this complication, we examined the role of NMDAR-CaMKII interactions in dendritogenesis using intermediate spinal cord cultures. These cultures uniquely function as natural "NR2 null neurons" that can form either synaptic NR1NR2A- or NR1NR2B-receptors when transducing the NR2A or NR2B subunits, respectively (Mi et al., 2004; Sepulveda et al., 2010). Consistent with results in intermediate hippocampal neurons, we found that NR2B-RS/QD expression impaired dendritogenesis in intermediate spinal cord neurons. Both the hippocampal and spinal cord neuron results strongly indicate that intermediate neurons require NR2B-NMDAR-CaMKII complexes for dendritogenesis.

Contrary to the findings in intermediate neurons (12 DIV), experiments with the tatCN21 peptide indicate that the NR2B-CaMKII interaction limits dendritogenesis in immature hippocampal neurons (5 DIV). What difference between the NR2B-NMDAR-CaMKII complexes in immature and intermediate hippocampal neurons could explain the opposing effects on dendritogenesis? We propose involvement of two different mechanisms: CaMKIIα-dependent GTPase Rem2 (Ghiretti et al., 2013) or CaMKIIβ (Fink et al., 2003). Regarding Rem2, studies in 5 DIV hippocampal neurons show that upon phosphorylation by CaMKII, Rem2 translocates to the nucleus, where it restricts dendritic complexity by suppressing CaMKIV signaling (Ghiretti et al., 2013). However, support for this idea remains lacking, and it should be determined if Rem2 remains coupled to CaMKIV nuclear signaling in more mature neurons.

Regarding CaMKII, the dodecameric CaMKII holoenzyme is comprised of either CaMKIIα isoforms (homomers) or CaMKIIα and β isoforms (heteromers) (Hell, 2014; Lisman et al., 2012). Surprisingly, the expression of CaMKIIβ, but not CaMKIIα, increases dendritic arborization in 5 DIV hippocampal neurons by regulating actin polymerization (Fink et al., 2003). Given that biochemical studies indicate that CaMKIIβ has a ~eightfold higher affinity for calcium/calmodulin than for CaMKIIα (Brocke, Chiang, Wagner, &

Schulman, 1999), and that CaMKIIα/NMDAR complexes exists under basal conditions (Leonard, Lim, Hemsworth, Horne, & Hell, 1999), it is plausible that, as for the mature neurons in slices (Sanhueza et al., 2011), the application of tatCN21 in immature neurons would reduce the interaction of NR2B-NMDARs with CaMKIIα in homomers or heteromers. In turn, this would allow for the calcium/CaM-dependent activation of β isoform-containing CaMKII holoenzymes that lead to actin-mediated dendritogenesis. Since CaMKIIβ is predominantly expressed during the first week of postnatal development in the hippocampus (Bayer, Löhler, Schulman, & Harbers, 1999), an uncoupling of NR2B-NMDAR-CaMKIIα complexes in older neurons would no longer activate actin polymerization and hence increase dendritogenesis.

Growing evidence supports that limited dendritic arbor complexity and consequently reduced synaptic connectivity play important roles in the memory impairments observed with aging and several neurological and cognitive disorders (Kulkarni & Firestein, 2012). An ongoing aim of the laboratory is to elucidate molecular mechanisms that might reactivate dendritogenesis. This has been challenging as dendrites stabilize in the mature neuronal circuitry (Chow et al., 2009; Koleske, 2013). In previous studies, we found that dendritogenesis could be reactivated in mature neurons by reducing synaptic PSD95 levels, which subsequently led to the reinsertion of extrasynaptic NR2B-NMDARs in mature synapses (Ampuero et al., 2017; Bustos et al., 2014). In the context of the data presented here, we suggest that reactivation of dendritogenesis in mature neurons by synaptically localized NR2B-NMDARs is mediated, at least in part, by the coupling of endogenous CaMKII to the NR2B C-terminal domain. The reduction of synaptic PSD95 levels in mature neurons leads to spine collapse and strong changes in synaptic transmission (Ampuero et al., 2017; Bustos et al., 2014; Ehrlich, Klein, Rumpel, & Malinow, 2007; Elias, Elias, Apostolides, Kriegstein, & Nicoll, 2008; El-Husseini et al., 2000; Losi et al., 2003; van Zundert et al., 2004). Additionally, the newly synaptically localized NR2B-NMDAR can induce excitoxicity (Liu et al., 2007). Not surprisingly, reduced PSD95 expression is reported in several human disorders, including in Alzheimer's disease, Huntington's disease, and schizophrenia (Arbuckle et al., 2010; de Bartolomeis, Latte, Tomasetti, & Iasevoli, 2014). To avoid this NR2B-NMDARs-dependent toxicity, we tested here if dendritogenesis could be reactivated when synaptically localized PSD95-NR2A complexes are coupled to CaMKII. Importantly, we showed here that expression of NR2AΔIN, a mutant NR2A construct with increased CaMKII interaction (Barria & Malinow, 2005; Gambrill & Barria, 2011; Mayadevi et al., 2002), reactivated dendritogenesis in mature hippocampal neurons in vitro and in vivo. In agreement with previous studies (Barria & Malinow, 2005; Gambrill & Barria, 2011), we did neither observe signs of excitoxicity nor spine collapse when neurons expressing NR2AΔIN. Mechanistically, our data indicate that reactivation of dendritogenesis in mature hippocampal neurons expressing NR2AΔIN is mediated by activation of the NMDAR/CaMKII/ERK-P/CREB-P signaling axis. The finding that global H3K27ac levels were not concomitantly increased in NR2AΔIN expressing neurons, unlike control neurons, is somewhat surprising. In future experiments, chromatin-immunoprecipitation assays coupled to whole-genome sequence analysis should give insights on whether control and NR2AΔIN expressing neurons display a differential enrichment of the H3K27ac mark on plasticity-related genes or other subsets of gene targets.

Conclusively, this work establishes that enhanced NR2A-NMDAR-CaMKII complex formation as a potential therapy to treat human neurological disorders where dendritic arbor complexity is limited, such as in depression, Alzheimer's disease, and stroke.

ACKNOWLEDGMENTS

We thank Fabiola Rojas and Luis Melo for their technical support. This work could not have been completed without the kind gifts of plasmid constructs from several investigators: NR2B-RS/QD and NR2AΔIN from Andres Barria; GFP-NR2A and GFP-NR2B from Stefano Vicini; NR2A-RNAi and NR2B-RNAi from Morgan Sheng and Myung Jong Kim. This work was supported by: Contract grant sponsor: FONDECYT; Contract grant number: 1140301 (to BvZ)—Contract grant sponsor: FONDECYT; Contract grant number: 1101012 (to BvZ)—Contract grant sponsor: UNAB Núcleus; Contract grant number: DI-603-14N (to BvZ)—Contract grant sponsor: DRI USA; Contract grant number: 2013–0030 (to BvZ)—Contract grant sponsor: FP7-PEOPLE-2011-IRSES; Contract grant number: 295185 (EULAMDIMA) (to BvZ, MM, JK)—Contract grant sponsor: FONDEQUIP; Contract grant number: EQM 140166 (to BvZ)—Contract grant sponsor: CONICYT; Contract grant number: 24110099 (to FB)— Contract grant sponsor: CONICYT; Contract grant number: 201161486 (to NJ)—Contract grant sponsor: FONDECYT; Contract grant number: 3130582 (to EA)—Contract grant sponsor: CONICYT; Contract grant number: 21151563 (to PM)—Contract grant sponsor: CONICYT; Contract grant number: 21151265 (to SA)—Contract grant sponsor: FONDECYT; Contract grant number: 11130203 (to MFT)—Contract grant sponsor: FONDECYT; Contract grant number: 1140700 (to MS)—Contract grant sponsor: FONDECYT; Contract grant number: 1150933 (to LVN)—Contract grant sponsor: FONDAP; Contract grant number: 15090007 (to MM)—Contract grant sponsor: FONDECYT; Contract grant number: 1130706 (to MM).

REFERENCES

Al-Hallaq, R. A., Conrads, T. P., Veenstra, T. D., & Wenthold, R. J. (2007). NMDA di-heteromeric receptor populations and associated proteins in rat hippocampus. *Journal of Neuroscience*, *27*, 8334–8343.

Alvarez, V. A., Ridenour, D. A., & Sabatini, B. L. (2007). Distinct structural and ionotropic roles of NMDA receptors in controlling spine and synapse stability. *Journal of Neuroscience*, *27*, 7365–7376.

Ampuero, E., Jury, N., Härtel, S., Marzolo, M.-P., & van Zundert, B. (2017). Interfering of the Reelin/ApoER2/PSD95 signaling axis reactivates dendritogenesis of mature hippocampal neurons. *Journal of Cellular Physiology*, *232*, 1187–1199.

Arbuckle, M. I., Komiyama, N. H., Delaney, A., Coba, M., Garry, E. M., Rosie, R., . . . Grant, S. G. N. (2010). The SH3 domain of postsynaptic density 95 mediates inflammatory pain through phosphatidylinositol-3-kinase recruitment. *EMBO Reports*, *11*, 473–478.

Bannister, A. J., & Kouzarides, T. (2011). Regulation of chromatin by histone modifications. *Nature Publishing Group*, *21*, 381–395.

Barria, A., & Malinow, R. (2005). NMDA receptor subunit composition controls synaptic plasticity by regulating binding to CaMKII. *Neuron*, *48*, 289–301.

Barrot, M., Olivier, J. D. A., Perrotti, L. I., DiLeone, R. J., Berton, O., Eisch, A. J., . . . Nestler, E. J. (2002). CREB activity in the nucleus accumbens shell controls gating of behavioral responses to emotional stimuli. *Proceedings of the National Academy of Sciences of the United States of America*, *99*, 11435–11440.

Bayer, K. U., De Koninck, P., Leonard, A. S., Hell, J. W., & Schulman, H. (2001). Interaction with the NMDA receptor locks CaMKII in an active conformation. *Nature*, *411*, 801–805.

Bayer, K. U., Löhler, J., Schulman, H., & Harbers, K. (1999). Developmental expression of the CaM kinase II isoforms: Ubiquitous gamma- and delta-CaM kinase II are the early isoforms and most abundant in the developing nervous system. *Brain Research Molecular Brain Research*, *70*, 147–154.

Bito, H., Deisseroth, K., & Tsien, R. W. (1996). CREB phosphorylation and dephosphorylation: A Ca(2+)- and stimulus duration-dependent switch for hippocampal gene expression. *Cell*, *87*, 1203–1214.

Brocke, L., Chiang, L. W., Wagner, P. D., & Schulman, H. (1999). Functional implications of the subunit composition of neuronal CaM kinase II. *Journal of Biological Chemistry*, *274*, 22713–22722.

Buard, I., Coultrap, S. J., Freund, R. K., Lee, Y.-S., Dell'Acqua, M. L., Silva, A. J., & Bayer, K. U. (2010). CaMKII "autonomy" is required for initiating but not for maintaining neuronal long-term information storage. *The Journal of Neuroscience*, *30*, 8214–8220.

Burt, A. M. (1980). Morphologic abnormalities in the postnatal differentiation of CA1 pyramidal cells and granule cells in the hippocampal formation of the ataxic mouse. *The Antanomical Record*, *196*, 61–69.

Bustos, F. J., Varela-Nallar, L., Campos, M., Henriquez, B., Phillips, M., Opazo, C., . . . van Zundert, B. (2014). PSD95 suppresses dendritic arbor development in mature hippocampal neurons by occluding the clustering of NR2B-NMDA receptors akaaboune M, ed. *PLoS ONE*, *9*, e94037.

Charych, E. I., Akum, B. F., Goldberg, J. S., Jörnsten, R. J., Rongo, C., Zheng, J. Q., & Firestein, B. L. (2006). Activity-independent regulation of dendrite patterning by postsynaptic density protein PSD-95. *The Journal of Neuroscience*, *26*, 10164–10176.

Chow, D. K., Groszer, M., Pribadi, M., Machniki, M., Carmichael, S. T., Liu, X., & Trachtenberg, J. T. (2009). Laminar and compartmental regulation of dendritic growth in mature cortex. *Nature Neuroscience*, *12*, 116–118.

Cline, H., & Haas, K. (2008). The regulation of dendritic arbor development and plasticity by glutamatergic synaptic input: A review of the synaptotrophic hypothesis. *The Journal of Physiology*, *586*, 1509–1517.

Cull-Candy, S. G., & Leszkiewicz, D. N. (2004). Role of distinct NMDA receptor subtypes at central synapses. *Sciences STKE*, *2004*, re16.

de Bartolomeis, A., Latte, G., Tomasetti, C., & Iasevoli, F. (2014). Glutamatergic postsynaptic density protein dysfunctions in synaptic plasticity and dendritic spines morphology: Relevance to schizophrenia and other behavioral disorders pathophysiology, and implications for novel therapeutic approaches. *Molecular Neurobiology*, *49*, 484–511.

Dunah, A. W., & Standaert, D. G. (2003). Subcellular segregation of distinct heteromeric NMDA glutamate receptors in the striatum. *Journal of Neurochemistry*, *85*, 935–943.

Dupuis, J. P., Ladépêche, L., Seth, H., Bard, L., Varela, J., Mikasova, L., . . . Groc, L. (2014). Surface dynamics of GluN2B-NMDA receptors controls plasticity of maturing glutamate synapses. *The EMBO Journal*, *33*, 842–861.

Ehrlich, I., Klein, M., Rumpel, S., & Malinow, R. (2007). PSD-95 is required for activity-driven synapse stabilization. *Proceedings of the National Academy of Sciences of the United States of America*, *104*, 4176–4181.

El-Husseini, A. E., Craven, S. E., Chetkovich, D. M., Firestein, B. L., Schnell, E., Aoki, C., & Bredt, D. S. (2000). Dual palmitoylation of PSD-95 mediates its vesiculotubular sorting, postsynaptic targeting, and ion channel clustering. *The Journal of Cell Biology*, *148*, 159–172.

Elias, G. M., Elias, L. A. B., Apostolides, P. F., Kriegstein, A. R., & Nicoll, R. A. (2008). Differential trafficking of AMPA and NMDA receptors by SAP102 and PSD-95 underlies synapse development. *Proceedings of the National Academy of Sciences of the United States of America*, *105*, 20953–20958.

Espinosa, J. S., Wheeler, D. G., Tsien, R. W., & Luo, L. (2009). Uncoupling dendrite growth and patterning: Single-Cell knockout analysis of NMDA receptor 2B. *Neuron*, *62*, 205–217.

Fink, C. C., Bayer, K.-U., Myers, J. W., Ferrell, J. E., Schulman, H., & Meyer, T. (2003). Selective regulation of neurite extension and synapse formation by the beta but not the alpha isoform of CaMKII. *Neuron*, *39*, 283–297.

Fortin, D. A., Davare, M. A., Srivastava, T., Brady, J. D., Nygaard, S., Derkach, V. A., & Soderling, T. R. (2010). Long-term potentiation-dependent spine enlargement requires synaptic Ca2+−permeable AMPA receptors recruited by CaM-kinase I. *The Journal of Neuroscience*, *30*, 11565–11575.

Foster, K. A., McLaughlin, N., Edbauer, D., Phillips, M., Bolton, A., Constantine-Paton, M., & Sheng, M. (2010). Distinct roles of NR2A and NR2B cytoplasmic tails in long-Term potentiation. *Journal of Neuroscience*, *30*, 2676–2685.

Gambrill, A. C., & Barria, A. (2011). NMDA receptor subunit composition controls synaptogenesis and synapse stabilization. *Proceedings of the National Academy of Sciences of the United States of America*, *108*, 5855–5860.

Gaudillière, B., Konishi, Y., la Iglesia de, N., Yao, G. L., & Bonni, A. (2004). A CaMKII-NeuroD signaling pathway specifies dendritic morphogenesis. *Neuron*, *41*, 229–241.

Ghiretti, A. E., Kenny, K., Marr, M. T., & Paradis, S. (2013). CaMKII-dependent phosphorylation of the GTPase Rem2 is required to restrict dendritic complexity. *The Journal of Neuroscience*, *33*, 6504–6515.

Gonçalves, J. T., Bloyd, C. W., Shtrahman, M., Johnston, S. T., Schafer, S. T., Parylak, S. L., . . . Gage, F. H. (2016). In vivo imaging of dendritic pruning in dentate granule cells. *Nature Neuroscience*, *19*, 788–791.

Greer, P. L., & Greenberg, M. E. (2008). From synapse to nucleus: Calcium-dependent gene transcription in the control of synapse development and function. *Neuron*, *59*, 846–860.

Hardingham, G. E., Chawla, S., Cruzalegui, F. H., & Bading, H. (1999). Control of recruitment and transcription-activating function of CBP determines gene regulation by NMDA receptors and L-type calcium channels. *Neuron*, *22*, 789–798.

Hell, J. W. (2014). CaMKII: claiming center stage in postsynaptic function and organization. *Neuron*, *81*, 249–265.

Henderson, C. E., Camu, W., Mettling C., Gouin A., Poulsen K., Karihaloo M., Rullamas J., Evans T., McMahon S. B., & Armanini M. P. (1993). Neurotrophins promote motor neuron survival and are present in embryonic limb bud. *Nature*, *363*, 266–270.

Henriquez, B., Bustos, F. J., Aguilar, R., Becerra, A., Simon, F., Montecino, M., & van Zundert, B. (2013). Ezh1 and Ezh2 differentially regulate PSD-95 gene transcription in developing hippocampal neurons. *Molecular and Cellular Neuroscience*, *57*, 130–143.

Jain, S., Yoon, S. Y., Zhu, L., Brodbeck, J., Dai, J., Walker, D., & Huang, Y. (2012). Arf4 determines dentate gyrus-mediated pattern separation by regulating dendritic spine development. *PLoS ONE*, *7*, e46340.

Jan, Y.-N., & Jan, L. Y. (2010). Branching out: Mechanisms of dendritic arborization. *Nature Reviews Neuroscience*, *11*, 316–328.

Kim, M. J., Dunah A. W., Wang Y. T., & Sheng M. (2005). Differential roles of NR2A- and NR2B-containing NMDA receptors in Ras-ERK signaling and AMPA receptor trafficking. *Neuron*, *46*, 745–760.

Koleske, A. J. (2013). Molecular mechanisms of dendrite stability. *Nature Reviews Neuroscience*, *14*, 536–550.

Kulkarni, V. A., & Firestein, B. L. (2012). The dendritic tree and brain disorders. *Molecular and Cellular Neuroscience*, *50*, 10–20.

Leonard, A. S., Lim, I. A., Hemsworth, D. E., Horne, M. C., & Hell, J. W. (1999). Calcium/calmodulin-dependent protein kinase II is associated with the N-methyl-D-aspartate receptor. *Proceedings of the National Academy of Sciences of the United States of America*, *96*, 3239–3244.

Lisman J., Yasuda R., Raghavachari S. (2012) Mechanisms of CaMKII action in long-term potentiation.:1–14.

Liu, Y., Wong, T. P., Aarts, M., Rooyakkers, A., Liu, L., Lai, T. W., . . . Wang, Y. T. (2007). NMDA receptor subunits have differential roles in mediating excitotoxic neuronal death both in vitro and in vivo. *Journal of Neuroscience*, *27*, 2846–2857.

Losi, G., Prybylowski, K., Fu, Z., Luo, J., Wenthold, R. J., & Vicini, S. (2003). PSD-95 regulates NMDA receptors in developing cerebellar granule neurons of the rat. *The Journal of Physiology*, *548*, 21–29.

Luo, J.-H., Fu, Z.-Y., Losi, G., Kim, B. G., Prybylowski, K., Vissel, B., & Vicini, S. (2002). Functional expression of distinct NMDA channel subunits tagged with green fluorescent protein in hippocampal neurons in culture. *Neuropharmacology*, *42*, 306–318.

Martin, S. J., Grimwood, P. D., & Morris, R. G. (2000). Synaptic plasticity and memory: An evaluation of the hypothesis. *Annual Review of Neuroscience*, *23*, 649–711.

Mayadevi, M., Praseeda, M., Kumar, K. S., & Omkumar, R. V. (2002). Sequence determinants on the NR2A and NR2B subunits of NMDA receptor responsible for specificity of phosphorylation by CaMKII. *Biochimica Et Biophysica Acta*, *1598*, 40–45.

Mi, R., Sia, G. M., Rosen, K., Tang, X., Moghekar, A., Black, J. L., . . . O'Brien, R. J. (2004). AMPA receptor-dependent clustering of synaptic NMDA receptors is mediated by Stargazin and NR2A/B in spinal neurons and hippocampal interneurons. *Neuron*, *44*, 335–349.

Molloy, S. S., & Kennedy, M. B. (1991). Autophosphorylation of type II Ca2+/calmodulin-dependent protein kinase in cultures of postnatal rat hippocampal slices. *Proceedings of the National Academy of Sciences of the United States of America*, *88*, 4756–4760.

Neve, R. L., Neve, K. A., Nestler, E. J., & Carlezon, W. A. (2005). Use of herpes virus amplicon vectors to study brain disorders. *Bio Techniques*, *39*, 381–391.

Nunez-Abades, P. A., & Cameron, W. E. (1995). Morphology of developing rat genioglossal motoneurons studied in vitro: Relative changes in diameter and surface area of somata and dendrites. *The Journal of Comparative Neurology*, *353*, 129–142.

Opazo, P., Labrecque, S., Tigaret, C. M., Frouin, A., Wiseman, P. W., De Koninck, P., & Choquet, D. (2010). CaMKII triggers the diffusional trapping of surface AMPARs through phosphorylation of stargazin. *Neuron*, *67*, 239–252.

Sanhueza, M., Fernandez-Villalobos, G., Stein, I. S., Kasumova, G., Zhang, P., Bayer, K. U., . . . Lisman, J. (2011). Role of the CaMKII/NMDA receptor complex in the maintenance of synaptic strength. *Journal of Neuroscience*, *31*, 9170–9178.

Sanhueza, M., & Lisman, J. (2013). The CaMKII/NMDAR complex as a molecular memory. *Molecular Brain*, *6*, 10.

Sans, N., Petralia, R. S., Wang, Y. X., Blahos, J., Hell, J. W., & Wenthold, R. J. (2000). A developmental change in NMDA receptor-associated proteins at hippocampal synapses. *Journal of Neuroscience*, *20*, 1260–1271.

Sanz-Clemente, A., Gray, J. A., Ogilvie, K. A., Nicoll, R. A., & Roche, K. W. (2013). Activated CaMKII couples GluN2B and casein kinase 2 to control synaptic NMDA receptors. *Cell Reports*, *3*, 607–614.

Sepulveda, F. J., Bustos, F. J., Inostroza, E., Zúñiga, F. A., Neve, R. L., Montecino, M., & van Zundert, B. (2010). Differential roles of NMDA Receptor Subtypes NR2A and NR2B in dendritic branch development and requirement of RasGRF1. *Journal of Neurophysiology*, *103*, 1758–1770.

Sfakianos, M. K., Eisman, A., Gourley, S. L., Bradley, W. D., Scheetz, A. J., Settleman, J., . . . Koleske, A. J. (2007). Inhibition of Rho via Arg and p190RhoGAP in the postnatal mouse hippocampus regulates dendritic spine maturation, synapse and dendrite stability, and behavior. *Journal of Neuroscience*, *27*, 10982–10992.

Shen, K., & Meyer, T. (1999). Dynamic control of CaMKII translocation and localization in hippocampal neurons by NMDA receptor stimulation. *Science*, *284*, 162–166.

Sheng, M., Cummings, J., Roldan, L. A., Jan, Y. N., & Jan, L. Y. (1994). Changing subunit composition of heteromeric NMDA receptors during development of rat cortex. *Nature*, *368*, 144–147.

Sheng, M., & Kim, E. (2011). The postsynaptic organization of synapses. *Cold Spring Harbor Perspectives in Biology*, *3*, a005678–a005678.

Tashiro, A., Sandler, V. M., Toni, N., Zhao, C., & Gage, F. H. (2006). NMDA-receptor-mediated, cell-specific integration of new neurons in adult dentate gyrus. *Nature*, *442*, 929–933.

Tovar, K. R., McGinley, M. J., & Westbrook, G. L. (2013). Triheteromeric NMDA receptors at hippocampal synapses. *Journal of Neuroscience*, *33*, 9150–9160.

van Zundert, B., Peuscher, M. H., Hynynen, M., Chen, A., Neve, R. L., Brown, R. H., . . . Bellingham, M. C. (2008). Neonatal neuronal circuitry shows hyperexcitable disturbance in a mouse model of the adult-onset neurodegenerative disease amyotrophic lateral sclerosis. *Journal of Neuroscience*, *28*, 10864–10874.

van Zundert, B., Yoshii, A., & Constantine-Paton, M. (2004). Receptor compartmentalization and trafficking at glutamate synapses: A developmental proposal. *Trends in Neurosciences*, *27*, 428–437.

Vest, R. S., Davies, K. D., O'Leary, H., Port, J. D., & Bayer, K. U. (2007). Dual mechanism of a natural CaMKII inhibitor. *Molecular Biology of the Cell*, *18*, 5024–5033.

West, A. E., Chen, W. G., Dalva, M. B., Dolmetsch, R. E., Kornhauser, J. M., Shaywitz, A. J., . . . Greenberg, M. E. (2001). Calcium regulation of neuronal gene expression. *Proceedings of the National Academy of Sciences of the United States of America*, *98*, 11024–11031.

West, A. E., & Greenberg, M. E. (2011). Neuronal activity-regulated gene transcription in synapse development and cognitive function. *Cold Spring Harbor Perspectives in Biology*, *3*, a005744–a005744

Wu, G. Y., & Cline, H. T. (1998). Stabilization of dendritic arbor structure in vivo by CaMKII. *Science*, *279*, 222–226.

Yashiro, K., & Philpot, B. D. (2008). Regulation of NMDA receptor subunit expression and its implications for LTD, LTP, and metaplasticity. *Neuropharmacology*, *55*, 1081–1094.

Zhao C, Teng EM, Summers RG, Ming G-L, Gage FH (2006) Distinct morphological stages of dentate granule neuron maturation in the adult mouse hippocampus. *Journal of Neuroscience 26*:3–11.

How to cite this article: Bustos FJ, Jury N, Martinez P, et al. NMDA receptor subunit composition controls dendritogenesis of hippocampal neurons through CAMKII, CREB-P, and H3K27ac. *J Cell Physiol*. 2017;232:3677–3692. https://doi.org/10.1002/jcp.25843